LV Challenge LKEB Contribution: Fully Automated Myocardial Contour Detection

Jeroen S. Wijnhout[1*], Dennis Hendriksen[1], Hans C. van Assen[2], Rob J. van der Geest[1]

[1]Division of Image Processing (LKEB), Department of Radiology, Leiden University Medical Center, PO BOX 9600, 2300 RC, Leiden, The Netherlands
[2] Biomedical Image Analysis, Biomedical Engineering, Eindhoven University of Technology, Eindhoven, The Netherlands
j.s.wijnhout@lumc.nl, d.hendriksen@lumc.nl, h.c.v.assen@tue.nl, rvdgeest@lumc.nl

Abstract. In this paper a contour detection method is described and evaluated on the evaluation data sets of the *Cardiac MR Left Ventricle Segmentation Challenge* as part of MICCAI 2009's *3D Segmentation Challenge for Clinical Applications*. The proposed method, using 2D AAM and 3D ASM, performs a fully automated detection of the myocardial contours, not requiring any user interaction. The algorithm's performance is reported using the metrics provided by the LV Challenge organization. Endocardial contour detection was classified as successful in 86% of the images and epicardial contours in 94%. The average perpendicular distance (APD) of the successful contours was 2.28 mm and 2.29 mm for the endo- and epicardial contours, respectively.

Introduction

In this paper a contour detection method is described and evaluated on the evaluation data sets of the *Cardiac MR Left Ventricle Segmentation Challenge* as part of MICCAI 2009's *3D Segmentation Challenge for Clinical Applications* [1]. The LV contour detection method described is composed of a pipeline of operations where the output of each stage is input to the next. In the setting of an application in which user-interaction is allowed, review and correction of the result of a particular stage may improve the final outcome of the algorithm. However, in the context of the LV Challenge our contribution concerns a fully automated detection approach. The details of the algorithm and the results obtained on the LV Challenge evaluation set are described in the next sections.

* J.S. Wijnhout was supported by Casimir grant 018.003.007 of the Netherlands Organization for Scientific Research (NWO).

Methods

Preparation

As initial preparation before applying fully automated contour detection, the two cardiac phases to be analyzed (i.e. ED and ES) and the image slices intersecting the LV were identified. The phase with a trigger delay closest to 300 ms was assumed to be the ES phase while the other phase was assumed to be the ED phase.

LV center point detection

The location and orientation of the long-axis of the left ventricle was identified using the Hough Transform for approximately circular objects [2]. For each of the images in the ED phase, the Hough Transform generates an accumulator image with identical dimensions as the input image, with high values near center points of objects having a radius within the specified range (2-60 mm). The range of radii was set large enough such that both endocardial and epicardial edge points would contribute to the automated determination of the ventricular center for a wide range of left ventricular sizes and cardiac pathologies. A straight line in 3D with maximum average intensity was fit through all available Hough accumulator images to estimate the long axis of the left ventricle. This procedure resulted in an estimation of the center of the left ventricle for each slice of the imaging study.

AAM based image segmentation

A 2D AAM based contour detection method similar as described by Mittchell et al [3] was used to obtain a first approximation of the LV endo- and epicardial and RV endocardial contours.

The AAM model used was trained on 40 cardiac MR data sets from different institutions including a variety of cardiac pathologies; all acquired on GE 1.5 T MR scanners [4]. For every study an experienced observer manually traced the LV endocardial and epicardial contours and RV endocardial contours in the ED and ES phases. The contour tracing protocol was similar to the one defined for the LV Challenge expert contours. No papillary muscle contours were identified. Separate AAM models were built for the ED and ES phases. Apical slices with a very small or no visual RV blood pool were excluded. For the most basal section, slices without complete circumference of LV myocardium were also excluded from the AAM training set. On average 5-6 ED slices and 4-5 ES slices were included for every dataset.

For AAM matching, the initial pose of the AAM was determined by the detected LV center point and the expected cardiac orientation derived from the image orientation information obtained from the DICOM image headers. The initial scale was chosen identical to the average cardiac size in the training set. AAM contour

detection was performed image by image, starting at a mid-ventricular slice. A conventional iterative matching procedure was followed minimizing the rms intensity difference between the model and the target image [3]. Improved robustness and computational efficiency was realized by propagating the found model parameters of a slice to initialize the model for neighboring slices. The matching process was performed for all ED and ES images and resulted in LV endocardial, epicardial and RV endocardial contours. These contours were used as input for the following contour detection steps.

Endocardial and epicardial contour detection

Despite the reported robustness of the AAM based contour detection approach, we have observed that the final result of the AAM method was deemed sub-optimal in various situations. First, since the metric minimized during the iterative fitting is global, the final contour location is often somewhat dislocated from the visually identified boundary even in cases where the boundary is depicted with high-contrast. This may partly be caused by the fact that the contour shape is too much constrained by statistical limits imposed by the model. Additionally, we have observed that for more complicated slices at the basal and apical level it occurs that during the fitting process the model fails to converge to a proper solution, which can lead to complete failures. This can be explained by the selection of images that was used for training the model, in which the most basal and apical slices were excluded. Finally, the iterative AAM matching process is sensitive to local minima, which may occasionally result in false contours.

Endocardial contour detection. The final endocardial contours were obtained using the algorithm described in [5]. In short, within the available epicardial contour an optimal threshold was determined separating the LV blood pool from the myocardium. A smooth convex shape (model contour) around the isolated blood pool was extracted, followed by dynamic programming, to obtain an endocardial contour fitting on the image gradients. In this step the search region was constrained to a small distance to the model contour.

Epicardial contour detection. Due to the variation in tissue characteristics of the region surrounding the myocardium, an edge based image detection technique, such as dynamic programming, can not be reliably applied for detection of the epicardial boundaries. Instead, we have applied a modified version of the *SPASM* algorithm described by van Assen et. al. [6]. This method uses a 3D Active Shape Model (ASM) which is fit on feature points detected by a fuzzy inference method. This method uses the Fuzzy C-Mean algorithm to classify pixels into three classes: blood/fat, myocardium and air. The 3D nature of this algorithm potentially results in better robustness, which is especially of importance for the detection in the basal and apical imaging sections.

As preparatory step image mis-registration artifacts due to breath-hold inconsistencies during image acquisition were reduced by aligning the short-axis images using the center of gravity of the previously detected endocardial contours.

This preparatory step is essential to make the short-axis data set a valid 3D scene. The initial position and orientation of the model was defined by the detected LV and RV contours.

The endocardial feature points were determined by the location of the detected endocardial contours, while the epicardial feature points were generated by applying the fuzzy inference method. The ASM model is divided into three sections: septal, lateral and apical. For each of the sections, fuzzy inference was applied. To this end image patches were sampled for which the location was determined by the available endocardial contours. The radial size of the patches was set to 20 mm multiplied by the LV size, computed from the AAM and dynamic programming contours, divided by the mean shape LV size. In the LV Challenge training set, the epicardial *good percentage* increased from 81% to 89% as a result of the *SPASM* detection while the APD and dice metric remained nearly the same. In cases where the epicardial detection failed, this was caused by incorrect endocardial contours.

RESULTS

Total processing time per study was 60 s on average, including reading the images and storing the contour files (Intel Core 2 Duo 2.2 GHz, single threaded).

Table 1 lists the number of endocardial and epicardial contours successfully detected for each of the 15 studies. On average 86% and 94% of the endo- and epicardial contours, respectively were detected within an average distance of 5 mm of the reference contours.

Table 1. Statistics for number of inner and outer contours per study and success rate of the automated contour detection algorithm.

	Number of Contours		**Detect Percentage**		**Good Percentage**	
ID	**Inner**	**Outer**	**Inner**	**Outer**	**Inner**	**Outer**
SC-HF-I-05	18	9	100	100	100	100
SC-HF-I-06	22	11	100	100	100	92
SC-HF-I-07	16	8	100	100	75	100
SC-HF-I-08	22	11	100	100	100	100
SC-HF-NI-07	24	12	100	100	92	100
SC-HF-NI-11	20	10	100	100	100	90
SC-HF-NI-31	18	10	95	100	84	100
SC-HF-NI-33	18	10	100	100	89	90
SC-HYP-06	13	7	100	100	85	100
SC-HYP-07	16	8	100	100	69	100
SC-HYP-08	19	10	100	100	68	90
SC-HYP-37	13	7	100	100	85	86
SC-N-05	15	8	100	100	80	100
SC-N-06	13	7	100	100	92	86
SC-N-07	18	10	100	100	78	80
Average	17.7	9.2	99.7	100	86.4	94.2
Stdev	3.4	1.6	1.4	0	11.0	7.0
Min	13	7	95	100	68.4	80
Max	24	12	100	100	100	100

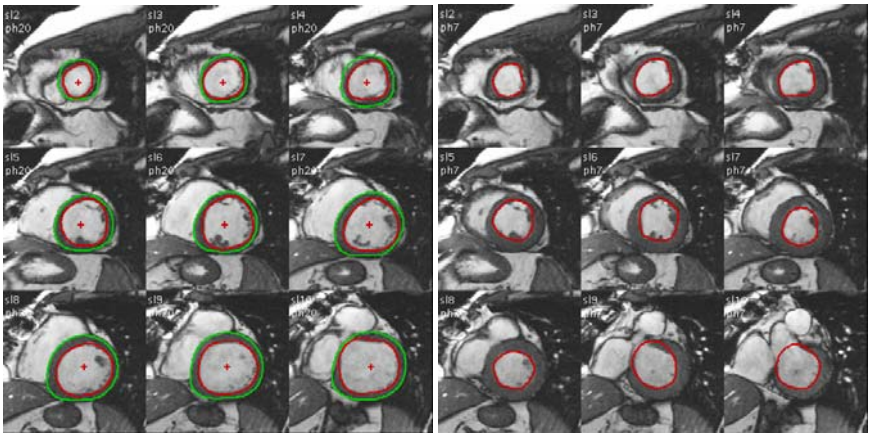

Fig. 1. Illustrative example of the result of automated contour detection for the images of study SC-HF-I-05 (case with the best APD score and Dice metric, left is ED, right is ES). APD is 1.7 mm for the inner and 1.6 mm for the outer contours. Ejection fraction was slightly overestimated by 4.6% while LV mass was underestimated by 4.4 g. Automatically detected center points are displayed in the ED images. Smoothness constraint applied in the endocardial detection algorithm results in contours surrounding the papillary muscles and trabeculations. However some overestimation occurred in the basal slices of the ES frame. Epicardial contour detection was successful for all slices of the ED phase.

Table 2. Results of APD and Dice metric.

	APD		Dice metric	
ID	**Inner**	**Outer**	**Inner**	**Outer**
SC-HF-I-05	1.7	1.6	0.94	0.96
SC-HF-I-06	1.8	2.4	0.92	0.94
SC-HF-I-07	2.8	2.2	0.88	0.93
SC-HF-I-08	2.1	2.3	0.92	0.93
SC-HF-NI-07	2.9	2.3	0.89	0.93
SC-HF-NI-11	2.3	2.0	0.91	0.95
SC-HF-NI-31	2.1	2.6	0.91	0.93
SC-HF-NI-33	2.3	2.9	0.87	0.91
SC-HYP-06	2.0	2.1	0.89	0.93
SC-HYP-07	2.2	2.4	0.90	0.93
SC-HYP-08	3.9	2.2	0.82	0.94
SC-HYP-37	2.3	3.0	0.83	0.90
SC-N-05	2.0	2.1	0.84	0.92
SC-N-06	2.1	1.7	0.89	0.94
SC-N-07	1.7	2.5	0.91	0.92
Average	2.29	2.28	0.89	0.93
Stdev	0.57	0.39	0.03	0.01
Min	1.67	1.57	0.82	0.90
Max	3.93	2.98	0.94	0.96

The APD and Dice metric values are listed in Table 2. The APD was similar for both contour types, being 2.29 mm and 2.28 mm for endo- and epicardial contours,

respectively. Dice metric values for both contour types were 0.89 for endocardial contours and 0.93 for epicardial contours. In general the results for the ED phase were better than for the ES phase. This is mainly caused by the influence of papillary muscles and trabeculations on the visibility of the myocardial boundaries.

The results of contour detection for the studies with the best and worst APD are illustrated in figure 1 and 2, respectively.

Table 3 lists the results of assessment of the LV ejection fraction and LV mass based on the automatically detected and the reference contours. The EF derived from automatically detected contours was not statistically significant different from the reference. LV mass was overestimated by 22.5g (18.9%) on average.

Table 3. Ejection fraction and LV mass evaluation obtained using PIC method (papillary muscles included in the LV blood pool)

	Ejection fraction (PIC)		**LV mass (PIC)**	
ID	**Reference**	**Auto**	**Reference**	**Auto**
SC-HF-I-05	33.03	37.67	115.45	111.04
SC-HF-I-06	25.78	28.64	147.34	177.83
SC-HF-I-07	28.18	19.84	114.12	117.12
SC-HF-I-08	21.42	26.27	124.40	179.53
SC-HF-NI-07	12.91	23.78	130.54	160.24
SC-HF-NI-11	14.84	22.82	158.25	203.80
SC-HF-NI-31	35.59	43.02	127.38	176.67
SC-HF-NI-33	58.35	63.84	130.78	182.49
SC-HYP-06	60.43	59.31	91.59	112.13
SC-HYP-07	62.27	45.98	133.55	182.25
SC-HYP-08	58.69	48.88	278.17	268.57
SC-HYP-37	71.68	67.29	125.38	93.02
SC-N-05	62.81	79.25	73.50	75.74
SC-N-06	54.59	58.57	64.02	80.94
SC-N-07	59.06	59.85	102.34	133.34
Average	44.0	45.7	127.8	150.3
Stdev	20.0	18.7	48.8	53.0
Min	12.9	19.8	64.0	75.7
Max	71.7	79.35	278.2	268.6
Signed difference		1.7±8.5 % (p=0.23)		22.5±26.2 g (p=0.0025) 18.9±20.0 %
Absolute difference		7.0±4.8 %		28.7±18.7 g 23.3±14.2 %

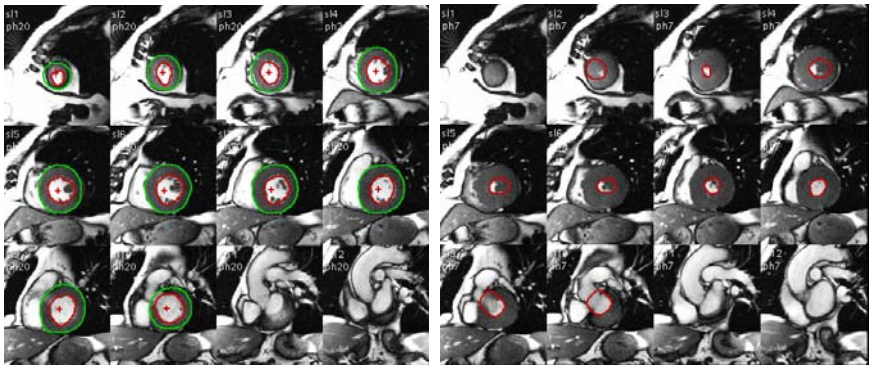

Fig. 2. Detection for the images of study SC-HYP-08 (case with lowest score; left is ED, right is ES). APD is 3.9 mm for the inner and 2.2 mm for the outer contours. Ejection fraction was underestimated by 9.8% while LV mass was slightly underestimated by 9.6 g (3.5 %). The low APD score for endocardial contours in mainly caused by failure of the algorithm to find the myocardial boundary in between the papillary muscles and trabeculations in the ES frame.

DISCUSSION

The described contour detection method was applied with reasonable success on the LV Challenge evaluation data. The training data supplied for the LV Challenge was used to test several contour detection approaches. The presented hybrid approach, in which an AAM based contour detection method was used as initial step followed by other techniques for the final contour detection resulted in the optimal APD and Dice metric values in the training set. No specific optimization of the algorithm parameters was performed on the type of data, although this might have resulted in some additional improvements. The limited set of 15 studies in the training set was also not sufficient to build a more specific AAM model for the LV Challenge sets. Instead it was decided to use a model which was trained on another set of GE MR data with characteristics slightly different from the LV Challenge data sets [4]. The resulting contours from the AAM detection step were used as valuable input for further processing using more image driven contour detection techniques. This is in line with a number of recent papers presenting LV contour detection algorithms heavily relying on image data rather than on a statistical or geometric models [7,8]. In general the quality of the data was such that the expert contours were located on strong edges in the images. However, this was not the case in a number of cases of hypertrophy patients where in the ES phase the endocardial contour was located in a region where papillary muscles and trabeculations were compressed together. In such cases a correct interpretation of the images is only possible by integrating knowledge of temporal variations. However, in our proposed algorithm information from temporal neighboring images was not used.

The evaluation of the performance of algorithm involved testing the method in a fully automated mode without applying any user interaction. The processing pipeline consists in a number of steps, in which every step in the processing is affected by the correctness of the result of the previous step. In a setting were user interaction is allowed, the user might first evaluate and correct any errors in the processing before proceeding with the next step. It is obvious that in such setting more accurate results may be obtained. For example, in the wrongly detected endocardial contour in the most apical ES slice in figure 2, would not have occurred if the user would have corrected the initially detected epicardial contour in this image.

In conclusion, we implemented a fully automated LV contour detection approach and successfully applied this algorithm on the LV Challenge evaluation data. Ejection fraction measurements derived from the automatically detected contour were in close agreement with expert results. LV mass measurements were over-estimated by on average 22.5%. However, by allowing a limited amount of user-interaction, the robustness of the developed approach can be significantly improved, resulting in a practical solution that can be implemented in clinical practice.

REFERENCES

1. Radau P, Lu Y, Connelly K, Paul G, Dick AJ, Wright GA. Evaluation Framework for Algorithms Segmenting Short Axis Cardiac MRI. The MIDAS Journal - Cardiac MR Left Ventricle Segmentation Challenge. http://hdl.handle.net/10380/3070.
2. Illingworth J.K.: A survey of the Hough transform. Computer Vision Graphics and Image Processing 44, 87-116 (1988).
3. Mitchell S.C., Lelieveldt B.P.F., van der Geest R.J., Bosch J.G., Reiber J.H.C., Sonka M.: Multistage hybrid active appearance model matching: Segmentation of left and right ventricles in cardiac MR images. IEEE Trans Med Imag 20, 415-423 (2001).
4. Angelié E., Oost E.R., Hendriksen D., Lelieveldt B.P.F., Van der Geest R.J., Reiber J.H.C.: Automated contour detection in cardiac MRI using active appearance models: the effect of the composition of the training set. Invest Radiol 42(10), 697-703 (2007).
5. van der Geest R.J., Buller V.G.M., Jansen E., Lamb H.J., Baur L.H.B., van der Wall E.E., de Roos A., Reiber J.H.C.: Comparison between manual and automated analysis of left ventricular volume parameters from short axis MR images. J Comput Assist Tomogr 21(5), 756-765 (1997).
6. van Assen H.C., Danilouchkine M.G., Frangi A.F., Ordás S., Westenberg J.J., Reiber J.H.C., Lelieveldt B.P.F.: SPASM: a 3D-ASM for segmentation of sparse and arbitrarily oriented cardiac MRI data. Med Image Anal 10(2), 286-303 (2006).
7. Cocosco C.A., Niessen W.J., Netsch T., Vonken E.J., Lund G., Stork A., Viergever M.A.: Automatic image-driven segmentation of the ventricles in cardiac cine MRI. J Magn Reson Imaging 28, 366-374 (2008).
8. Codella N.C., Weinsaft J.W., Cham M.D., Janik M., Prince M.R., Wang Y.: Automated segmentation by using myocardial effusion threshold reduction and intravoxel computation at MR imaging. Radiology 248, 1004-1012 (2008).